International Immunopharmacology 75 (2019) 105752

Contents lists available at ScienceDirect

International Immunopharmacology

journal homepage: www.elsevier.com/locate/intimp

Adenovirus-mediated transduction with *Histone Deacetylase 4* ameliorates disease progression in an osteoarthritis rat model

Xiao-dong Gu[a], Lei Wei[b], Peng-cui Li[a], Xian-da Che[a], Rui-peng Zhao[a], Peng-fei Han[a], Jian-gong Lu[a], Xiao-chun Wei[a,*]

[a] Department of Orthopaedics, The Second Hospital of Shanxi Medical University, Shanxi Key Laboratory of Bone and Soft Tissue Injury Repair, Taiyuan, Shanxi, PR China
[b] Department of Orthopedics, Warren Alpert Medical School of Brown University, Providence, RI, USA

ARTICLE INFO

Keywords:
Histone deacetylase 4
Rat chondrocyte
Anterior cruciate ligament transection (ACLT)
Osteoarthritis (OA)
Adenovirus vector

ABSTRACT

Background: Downregulation of histone deacetylase-4 (HDAC4) contributes to cartilage degeneration in osteoarthritis (OA) because it promotes upregulation of runt-related transcription factor-2 (Runx-2) and osteoarthritis-related genes. The effect of HDAC4 upregulation on cartilage damage in OA remains unknown.
Methods: Rat chondrocytes were infected with Ad-*GFP* or Ad-*HDAC4-GFP* for 48 h, stimulated with interleukin-1β (IL-1β, 10 ng/mL) for 24 h, and then harvested for RT-qPCR. Male Sprague-Dawley rats in 3 groups were given anterior cruciate ligament transection (ACLT) or sham operation, and knee injections with different adenovirus (Ad) vectors at 48 h after surgery and every 3 weeks thereafter: ACLT + Ad-*GFP* (n = 17); ACLT + Ad-*HDAC4-GFP* (n = 20); and sham + Ad-*GFP* (n = 15). Three ACLT-Ad-*HDAC4-GFP* rats were sacrificed at different times to examine the expression of HDAC4. Two ACLT-Ad-*GFP* rats and two ACLT-Ad-*HDAC4-GFP* rats were euthanized at week-2; articular cartilage was harvested and expression of *HDAC4* was determined by RT-qPCR. All other rats were euthanized at week-8. Cartilage damage and OA progression was assessed using radiography, fluorescence molecular tomography (FMT), histology, immunohistochemistry (IHC), ELISA, and RT-qPCR.
Results: Overexpression of HDAC4 in chondrocytes stimulated by IL-1β reduced the levels of *Runx-2*, *MMP-13*, and *Collagen X*, but increased the levels of *Collagen II* and *Aggrecan*. Upregulation of *HDAC4* reduced osteophyte formation and cartilage damage, and increased articular cartilage anabolism.
Conclusion: HDAC4 attenuated articular cartilage damage by repression of Runx-2, MMP-13, and collagen X and induction of collagen II and ACAN in this rat model of OA. Upregulation of HDAC4 may provide chondroprotection in OA patients.

1. Introduction

Osteoarthritis (OA) is the most common joint disease among the elderly and is associated with tremendous individual and socio-economic burdens [1,2]. A recent survey reported that OA is the major cause of knee joint dysfunction in the aged [3]. The main pathological changes associated with OA are progressive disruption within the articular cartilage and osteophyte formation, and these can cause chronic pain and dysfunction in affected joints. The molecular pathogenesis of OA is not completely understood, and there are currently no effective pharmacological therapies for prevention or treatment.

Recent studies demonstrated that chondrocytes enter hypertrophic differentiation during the early-stage of OA [4,5]. These hypertrophic chondrocytes express increased levels of Runt-related transcription factor 2 (Runx-2), matrix metalloproteinase-13 (MMP-13), type X collagen (Col X), and Indian hedgehog (IHH), leading to an imbalance of anabolism and catabolism in the cartilage and to cartilage destruction [6–8]. Runx-2 and MMP-13 are the most significant of these hypertrophic factors. Runx-2 is a critical regulator for chondrocyte hypertrophy [9,10]. MMP-13 plays a significant role in the degradation of cartilage extracellular matrix (ECM) and degrades cartilage ECM directly during the initial stages of OA [11]. At the molecular level, MMP-13 efficiently degrades type II collagen (Col II) [12]. Therefore, repression of chondrocyte hypertrophy might help to attenuate or reverse articular cartilage degradation in OA. However, the impact of selectively decreasing the expression of Runx-2, MMP-13, and Col X on OA is unclear.

Histone deacetylase 4 (HDAC4) belongs to the class IIa histone deacetylase family and mainly occurs in the brain, muscle, and cartilage [13,14]. HDAC4 represses chondrocyte hypertrophy and the expression

* Corresponding author at: The Second Hospital of Shanxi Medical University, 382 Wuyi Road, Taiyuan 030001, PR China.
E-mail address: sdeygksys@163.com (X.-c. Wei).

https://doi.org/10.1016/j.intimp.2019.105752
Received 23 May 2019; Received in revised form 21 June 2019; Accepted 10 July 2019
Available online 13 July 2019

of MMP-13 by inhibiting the activity of Runx-2 [15]. Hdac4$^{-/-}$ mice have increased expression of MMP-13 in hypertrophic chondrocytes [16]. Evidence from our laboratory indicated a lower level of HDAC4 in cartilage from OA patients than in cartilage from healthy donors, and up-regulation of Runx-2, MMP-13, and Col X in OA patients [17]. Our *in vitro* experiments also indicated that HDAC4 inhibits the transcription of Runx-2 and MMP-13 by repressing their promoter activities [17]. Thus, the upregulation of HDAC4 appears to have a chondroprotective effect by inhibiting the transcription of Runx-2 and MMP-13, and may therefore be useful as a therapy for OA.

To investigate this hypothesis, we first used rat costal chondrocytes to investigate the *in vitro* effects of *HDAC4*. We then performed an *in vivo* study using an established OA rat model, induced by knee joint anterior cruciate ligament transection (ACLT), in which an adenoviral vector was used to upregulate *HDAC4* in the knee cartilage.

2. Materials and methods

This study was approved by the Animal Ethics Committee of Shanxi Medical University (approval project identification code: 2016LL083, March 14, 2016). All procedures on animals were in compliance with the animal protection agreements and regulations.

2.1. Construction of adenoviral vectors

An adenoviral vector encoding *HDAC4* and *green-fluorescent protein* (Ad-*HDAC4-GFP*) and a negative control (Ad-*GFP*) were constructed and purified by Genechem (GCPA0154814, Shanghai, China). The virus titer was 1×10^9 plaque-forming units (PFUs)/mL for *in vitro* experiments, and the titer was 1×10^9 PFUs per knee for *in vivo* experiments.

2.2. Chondrocyte culture

Costal chondrocytes were isolated from neonatal Sprague-Dawley (SD) rat as described previously [18] and cultured in Dulbecco's Modified Eagle's Medium (Hyclone) supplemented with 10% fetal bovine serum (Hyclone). At passage 2, the chondrocytes were seeded in 6-well plates and stimulated with 10 ng/mL IL-1β (PeproTech) for 24 h. Untreated cells were used as controls. To investigate the effects of *HDAC4 in vitro*, the chondrocytes were infected with 200 multiplicities of infection (MOI) of *Ad-GFP* or *Ad-HDAC4-GFP* for 48 h; this MOI led to an infection efficiency of nearly 100% and high cell viability. The cells were then stimulated with 10 ng/mL IL-1β for 24 h, and then harvested for real-time quantitative PCR (RT-qPCR).

2.3. Rat anterior cruciate ligament transection (OA model) and HDAC4 gene delivery

Eight-week-old male Sprague-Dawley (SD) rats (n = 52) were purchased from Shanxi Medical University. OA was induced by anterior cruciate ligament transection (ACLT), and the rats were then randomly divided into 3 groups: ACLT + Ad-*GFP* (henceforth, Ad-*GFP*; n = 17), ACLT + Ad-*HDAC4-GFP* (henceforth, Ad-*HDAC4*; n = 20), and sham-operated + Ad-*GFP* (henceforth, sham-operated; n = 15). The operations were performed on the right knees, as described previously [19]. Ad-*HDAC4-GFP* and Ad-*GFP* were administered by intra-articular injection 48 h after surgery, and every 3 weeks thereafter. Three rats from the Ad-*HDAC4* group were sacrificed at 3 days, 2 weeks, and 3 weeks after the initial adenovirus injection for histological examination of 5-μm sections to determine the location and expression of HDAC4 in the rat knee and tibial plateau using fluorescence microscopy. Two rats from the Ad-*GFP* group and 2 rats from the Ad-*HDAC4* group were sacrificed 2 weeks after the initial adenovirus injection; the articular cartilage was harvested, and the expression of *HDAC4* was examined by RT-qPCR. All other animals were euthanized 8 weeks after surgery.

2.4. Radiography

A small-animal X-ray apparatus (Faxitron UltraFocus, Arizona, USA) was used to evaluate radiographic changes in the rat knee at 8 weeks after surgery. X-rays were taken with rats in the anteroposterior and lateral positions while under anesthesia. The exposure time and kV settings were set at “full AUTO”.

2.5. Fluorescence molecular tomography

Fluorescence molecular tomography (FMT) is a sensitive and quantitative technology that provides *in vivo* 3-dimensional tissue imaging [20,21]. FMT (FMT 4000 *In Vivo* Imaging System, PerkinElmer, Waltham, MA, USA) was used to monitor the levels of MMPs in rat knees at 8 weeks after surgery. The rats received intra-articular injections with a single dose of MMPSense 645 FAST Fluorescent Imaging Agent (20 μL, 0.8 nmol; PerkinElmer) 24 h before imaging. MMPSense 645 FAST is a matrix metalloproteinase (MMP)-activatable agent that emits fluorescence after cleavage by multiple MMPs *in vivo* (including MMP-2, −3, −7, −9, −12, and − 13). The concentrations of the MMPs probes in the rat knee were calculated using the region of interest (ROI) method. Data are presented as means ± standard deviations (SDs), with 5 rats per group.

2.6. Histology

Gross morphologic lesions on the femoral condyle and tibial plateau in rats (3 per group) were visualized by India ink staining. The proximal tibiae (12 per group) were harvested from the right knee joints and fixed in 4% paraformaldehyde for 48 h. The tibial plateaus were decalcified in a 10% EDTA solution for 8 weeks, and each one was cut into 2 approximately equal pieces along the frontal plane. Each half was embedded in a paraffin block, and frontal sectioning was performed. Ten 5-μm sections were obtained at three 200-μm intervals (total of 60 sections), and two sections from each interval were stained with Safranin O/Fast Green. The Osteoarthritis Research Society International (OARSI) grading system was used to quantify cartilage degradation [22]. This score ranges from 0 to 24, and a higher score indicates more degeneration. Three independent and blinded observers scored each section, and the scores from the proximal tibiae sections were averaged for each rat.

2.7. Immunohistochemistry

Col II, Col X, MMP-13, and Runx-2 were visualized using immunohistochemistry (IHC). The slides were first dewaxed with xylene and then rehydrated with graded ethanol. Endogenous peroxidase activity was quenched with an endogenous peroxidase block for 10 min at room temperature. For antigen retrieval, 0.1% trypsin was used to digest the sections at 37 °C for 30 min and then incubated with a primary antibody against rat Col II (ab34712; Abcam), Col X (BA2023; Boster, Wuhan, China), Runx-2 (ab23981; Abcam), or MMP-13 (ab39012; Abcam) at 4 °C overnight. The sections were then incubated with horse radish peroxidase (HRP)-conjugated secondary antibody for 30 min at 37 °C and developed using a 3,3′-diaminobenzidine chromogen. Photographs were taken with a Leica DM6B microscope (Leica, Wetzlar, Germany).

2.8. Enzyme-linked immunosorbent assay

Rat knee synovial fluid (SF) was collected by lavage, as described previously [23], prior to analysis by an enzyme-linked immunosorbent assay (ELISA). First, 100 μL of an isotonic saline solution was administered by intra-articular injection into the rat knee joint using a microscale syringe. The knee was then passively flexed and extended 20 times to distribute the fluid within the joint before aspiration. About

40 μL of lavage was then collected, centrifuged for 10 min at 2000*g* to remove cells and particulates, and stored at −80 °C until analysis. The MMP-13 concentration was measured using ELISA, according to the manufacturer's protocol (Bioswamp, China). A_{450nm} of the developed plates was measured using a microplate reader (SpectraMax M5; Molecular Devices, USA). ELISA analysis of each sample was performed in duplicate.

2.9. RT-qPCR

Total RNA was isolated from chondrocytes and rat articular cartilage using the TRIzol™ Reagent (Invitrogen). The femoral condyle cartilage was dissected using a scalpel and then ground in liquid nitrogen. Cartilage samples from 4 rats were then pooled together, with 3 pooled samples per group. Isolated RNA was reverse-transcribed into complementary DNA (cDNA) using PrimeScript™ RT Master Mix, and RT-qPCR was performed using TB Green™ Premix Ex Taq™ II with the Applied Biosystems™ QuantStudio™ 6 Flex Real-Time PCR System. The RT-qPCR conditions were 95 °C for 30 s, followed by 40 cycles of 95 °C for 5 s, and 60 °C for 30 s, and then dissociation (95 °C for 15 s, 60 °C for 60 s, and 95 °C for 15 s) after the amplification procedure. Relative transcript levels were calculated using the $2^{-\Delta\Delta Ct}$ method, as previously described [24]. The primer sequences are given in Table 1.

2.10. Statistical analysis

Data are expressed as means ± standard deviations (SDs). A one-way analysis of variance (ANOVA) was used to analyze the differences in mean OARSI scores, FMT results, MMP-13 concentrations, and mRNA levels of *Runx-2*, *MMP-13*, *Col X*, *Col II*, and *ACAN*. The least significant difference (LSD) multiple comparisons test was used for pairwise comparisons following ANOVA. A difference was considered significant if the P value was < 0.05. The statistical analyses were performed using SPSS version 19.0.

3. Results

3.1. HDAC4 inhibits IL-1β-stimulated catabolism of rat chondrocytes

Our fluorescence microscopy results show successful *in vitro* adenovirus-mediated *HDAC4* infection of rat chondrocytes, as indicated by strong green fluorescence at 48 h (Fig. 1A). In addition, RT-qPCR of uninfected chondrocytes showed that stimulation with IL-1β increased the expression of *Runx-2*, *MMP-13* and *col X*, but decreased the expression of *Col II* (Fig. 1B). Relative to the controls (Ad-*GFP* infected cells), infection of chondrocytes with *HDAC4* reduced the levels of *Runx-2*, *MMP-13*, and *Col X* induced by IL-1β, and increased the expression of *Col II* and *Aggrecan* (Fig. 1C).

Table 1
Sequences of primers.

Gene	Sequence (5′-3′)
rat *HDAC4*	F: GGCTTCCTTGTGGTGGTGTTGG R: TGTACTCTCCTCGGCATGGTGTC
rat *Col2a1*	F: GAGGGCAACAGCAGGTTCAC R: TGTGATCGGTACTCGATGATGG
rat *ACAN*	F: CTGATCCACTGTCCAAGCACCATG R: ATCCACGCCAGGCTCCACTC
rat *Col10a1*	F: GGATGCCTCTTGTCAGTGCTAACC R: TCATAGTGCTGCTGCCTGTTGTAC
rat *MMP-13*	F: AACCAGATGTGGAGTGCCTG ATG R:CACATCAGACCAGACCTTGAAGGC
rat *Runx-2*	F: AACAGCAGCAGCAGCAGCAG R: GCACGGAGCACAGGA AGTTGG
18S rRNA	F: CGGCTACCACATCCA AGGAA R: GCTGGA ATTACCGCGGCT

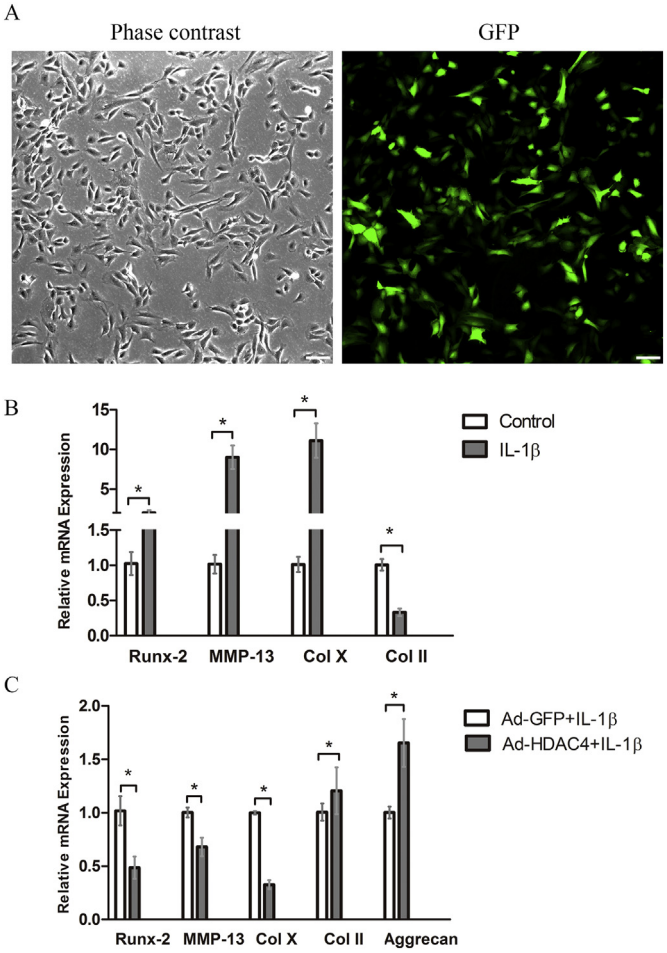

Fig. 1. Effect of Ad-*HDAC4* on *in vitro* catabolism of rat chondrocytes stimulated by IL-1β. (**A**) Rat chondrocytes had strong green fluorescence 48 h after infection with 200 MOI Ad-*HDAC4-GFP*. Scale bars: 100 μm (**B**) RT-qPCR of uninfected chondrocytes show increased levels of *Runx-2*, *MMP-13*, and *Col X* and decreased levels of *Col II* at 24 h after stimulation with 10 ng/mL IL-1β. (**C**) Overexpression of *HDAC4* reduced the levels of *Runx-2*, *MMP-13*, and *Col X* induced by IL-1β in rat chondrocytes and increased the levels of *Col II* and *Aggrecan*. Here and below: * indicates $P < 0.05$. (For interpretation of the references to color in this figure legend, the reader is referred to the web version of this article.)

3.2. Adenovirus-mediated transduction of HDAC4 into articular cartilage of rat knees

We successfully introduced the *HDAC4* gene into the rat articular cartilage, as indicated by green fluorescence at day 3 (Supplementary Materials Fig. 1A). This fluorescence signal was stronger at 2 weeks, but much weaker at 3 weeks. At 2 weeks after injection, articular cartilage was collected for measurement of *HDAC4* mRNA by RT-qPCR. The results showed that the *HDAC4* mRNA was 8.87-fold higher in the Ad-*HDAC4* group than in the Ad-*GFP* group (Supplementary Materials Fig. 1B).

3.3. Radiology indicates that HDAC4 alleviates overt changes in OA

We evaluated overt changes of OA in knees by taking radiographs at 8 weeks after ACLT (Fig. 2). The results indicated osteophyte formation along the patella, tibial plateau, and tibial intercondylar eminence in the Ad-*GFP* group. Although some osteophytes were also present in the Ad-*HDAC4* group, they were less evident. There was no evident osteophyte formation in the sham-operated group.

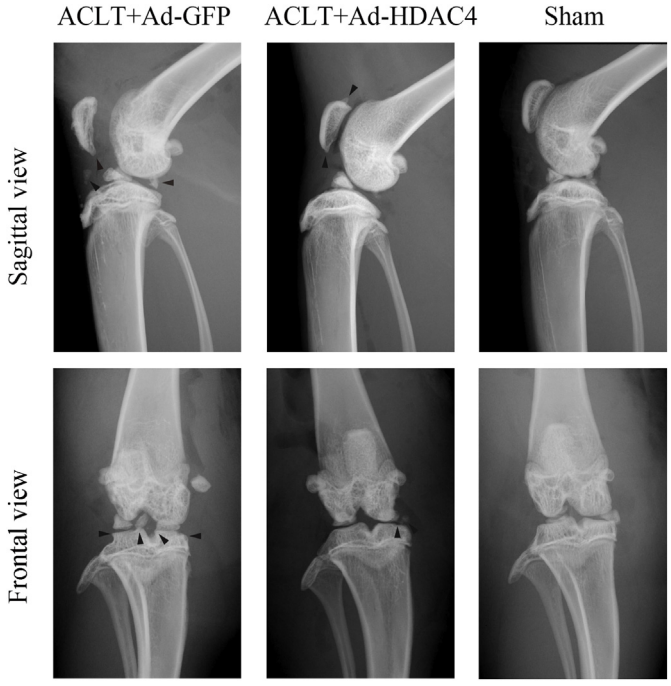

Fig. 2. Sagittal and frontal osteophyte formation of the knee of a rat model of OA at 8 weeks after surgery. X-rays show greater changes in osteophyte formation along the patella, tibial plateau, and tibial intercondylar eminence in the Ad-*GFP* group than in the Ad-*HDAC4* group (black arrow heads). The sham-operated group had no evidence of osteophyte formation.

3.4. Histology indicates that HDAC4 attenuates severity of cartilage degeneration in OA

We also examined gross morphologic lesions using India ink staining, in which more staining indicates more severe cartilage destruction (Fig. 3A). The results show that the femoral condyle and tibial plateau cartilage had more staining in the Ad-*GFP* group than in the Ad-*HDAC4* and the sham-operated group (which had no staining). The Ad-*HDAC4* group also had a smoother cartilage surface and less cartilage erosion than the Ad-*GFP* group.

We stained the articular cartilage with Safranin O, which stains for proteoglycans and glycosaminoglycans and indicates cartilage surface disruption (Fig. 3B). The results show weak Safranin O staining in the Ad-*GFP* group but strong staining, more cellularity, more intact cartilage surface, and less fibrillation in the Ad-*HDAC4* group. The resulting OARSI scores were significantly higher in the Ad-*GFP* group (14.31 ± 2.56) than in the Ad-*HDAC4* group (9.53 ± 1.88; $P < 0.05$). Rats in the sham-operated group had the lowest OARSI scores (0.47 ± 0.45; $P < 0.05$; Fig. 3C).

3.5. IHC indicates that HDAC4 promotes anabolism and inhibits catabolism of cartilage

We compared the 3 groups using IHC staining of articular cartilage (Fig. 4). The results show greater Col II staining in the Ad-*HDAC4* and sham-operated groups than in the Ad-*GFP* group. In contrast, Col X, Runx-2, and MMP-13 staining were significantly greater in the Ad-*GFP* group than in the Ad-*HDAC4* and sham-operated group. ELISA of joint lavage fluid confirmed the IHC results for MMP-13 (Fig. 4E). In particular, the Ad-*GFP* group had an MMP-13 concentration of 21.97 ± 0.79 ng/mL, higher than the Ad-*HDAC4* group (16.38 ± 0.59 ng/mL; $P < 0.05$) and the sham-operated group (12.46 ± 1.03 ng/mL; $P < 0.05$).

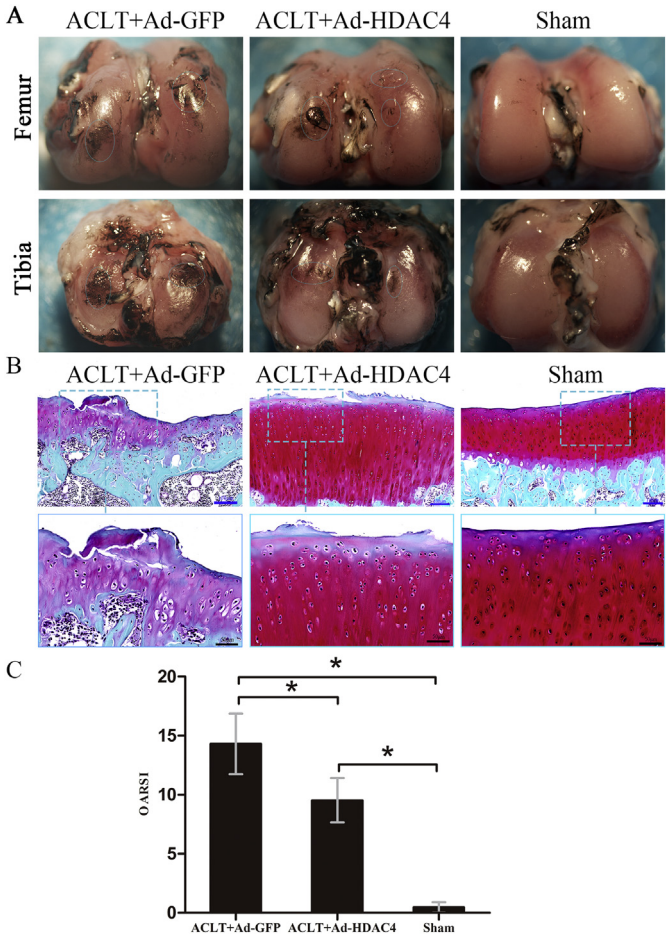

Fig. 3. Effect of Ad-*HDAC4* on disease progression in a OA rat model at 8 weeks after surgery. (**A**) India ink staining after transduction shows the Ad-*HDAC4* group had less staining and a smoother surface than the Ad-*GFP* group. (**B**) The Ad-*HDAC4* group also had stronger staining than the Ad-*GFP* group for Safranin O. The bottom panels are higher-magnification views of the boxed areas in the top panels. Blue scale bars: 100 μm; black scale bars: 50 μm. (**C**) OARSI scores indicated less cartilage damage in the Ad-*HDAC4* group than in the Ad-*GFP* group, and little or no cartilage damage in the sham-operated group. (For interpretation of the references to color in this figure legend, the reader is referred to the web version of this article.)

3.6. RT-qPCR indicates that HDAC4 promotes anabolism and inhibits catabolism of cartilage

We performed real-time qPCR to confirm the IHC experiments (Fig. 5). These results indicate that, relative to the Ad-*GFP* group, the Ad-*HDAC4* group had lower levels of *Runx-2*, *MMP-13*, and *Col X*, but increased levels of *Col II* and *ACAN*. In addition, relative to the Ad-*HDAC4* group, the sham-operated group had lower levels of *Runx-2*, *MMP-13*, and *Col X*, but increased levels of *Col II* and *ACAN*.

3.7. FMT shows that HDAC4 decreases MMP levels

We analyzed living rats using FMT with appropriate probes to monitor the levels of total MMPs in the knee (Fig. 6). The results show that MMP levels were significantly lower in the Ad-*HDAC4* group (23.47 ± 2.00 pmol) and sham-operated group (5.27 ± 1.49 pmol) than in the Ad-*GFP* group (39.87 ± 3.76 pmol; $P < 0.05$). These results are consistent with the above results from IHC, RT-qPCR, and ELISA.

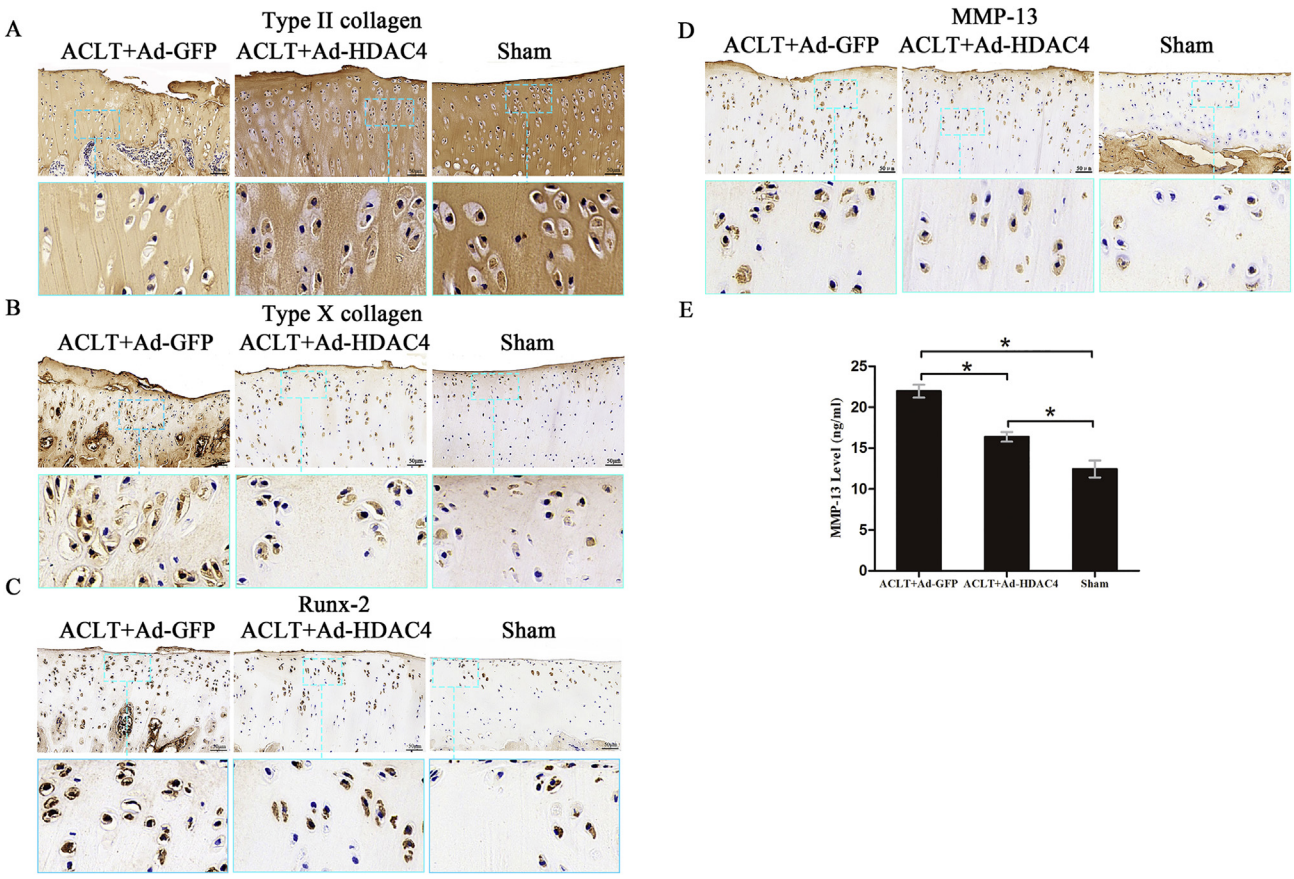

Fig. 4. IHC staining for markers of cartilage catabolism and anabolism in a rat model of OA at 8 weeks after surgery. (**A**) Col II staining was greater in the Ad-*HDAC4* and sham-operated groups than in the Ad-*GFP* group. (**B**, **C**, and **D**) Col X, Runx-2, and MMP-13 staining was greater in the Ad-*GFP* group than in the other two groups. The bottom panels are higher-magnification views of the boxed areas in the top panels. Scale bar: 50 μm. (**E**) The Ad-*HDAC4* group had a lower concentration of MMP-13 in SF than rats in the Ad-*GFP* group, and the sham-operated group had the lowest level.

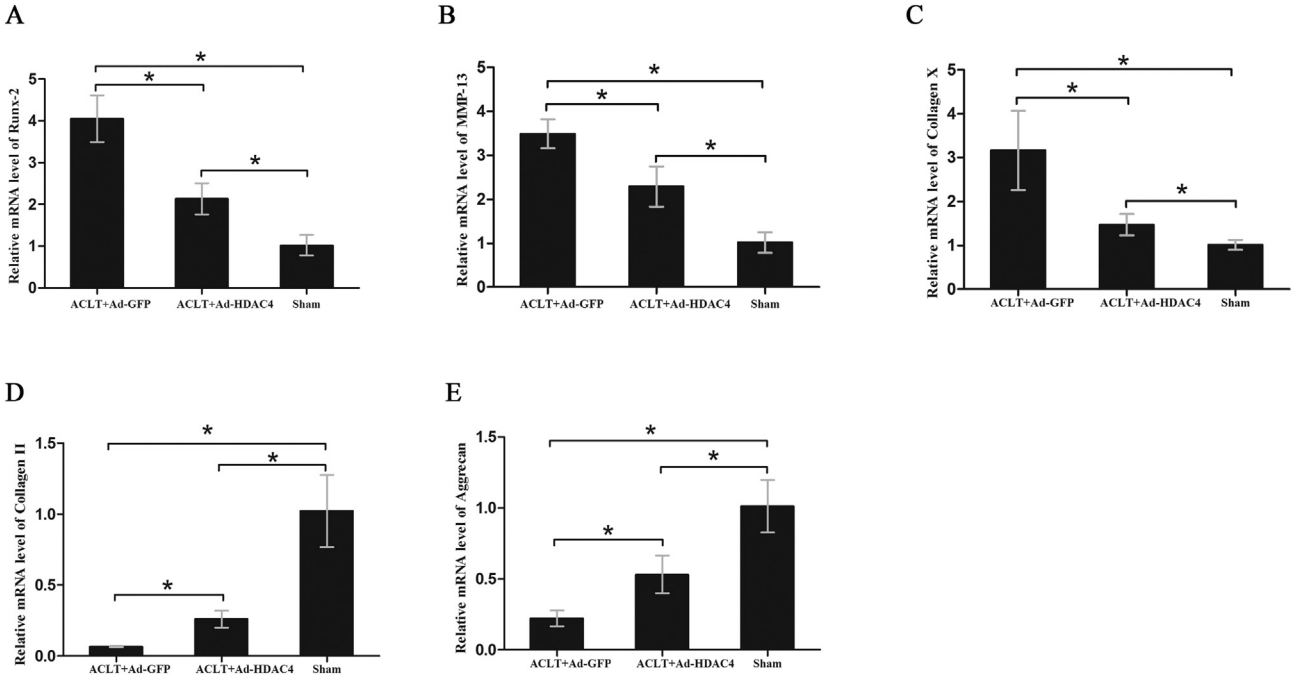

Fig. 5. RT-qPCR of markers of cartilage catabolism and anabolism in a rat model of OA at 8 weeks after surgery. (**A**, **B**, and **C**) The Ad-*HDAC4* group, relative to the Ad-*GFP* group, had reduced expression of *Runx-2*, *MMP-13*, and *Col X*, and the sham-operated group had the lowest levels of all 3 genes. (**D** and **E**) The Ad-*HDAC4* group, relative to the Ad-*GFP* group, had greater expression of *type II collagen* and *ACAN*, and the sham-operated group had the highest levels of both genes.

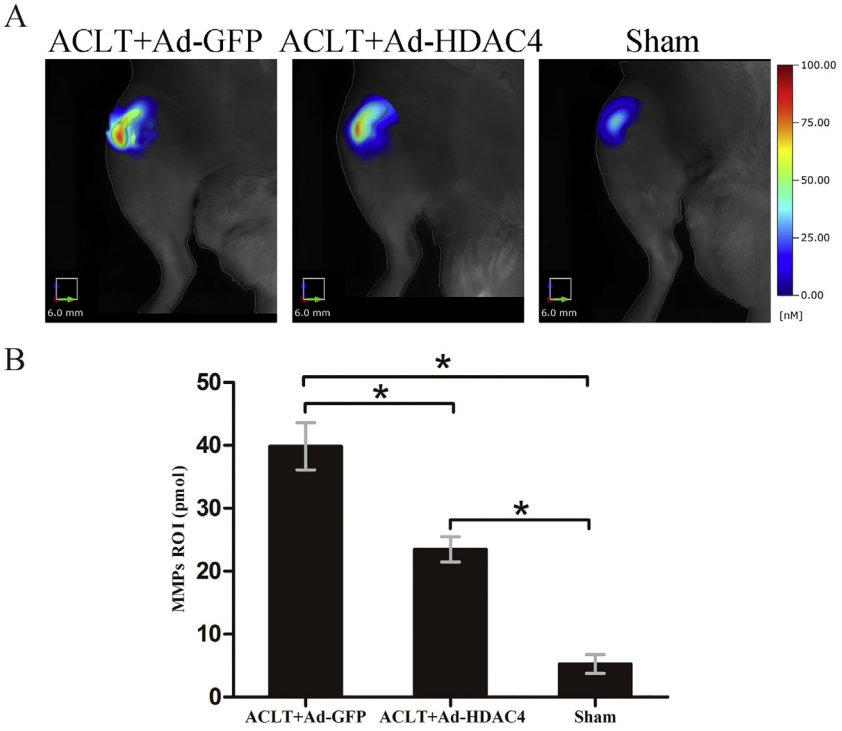

Fig. 6. FMT measurement of total MMPs in a rat model of OA at 8 weeks after surgery. (**A**) The Ad-*HDAC4* group had a lower level of MMPs than the Ad-*GFP* group, and the sham-operated group had the lowest level. (**B**) Quantitation of results in the regions of interest (5 rats per group).

4. Discussion

HDAC4 represses chondrocyte hypertrophy by inhibiting the activity of Runx-2, a transcription factor necessary for this process. Thus, a previous *in vivo* study demonstrated that *HDAC4*-null mice developed precocious mineralization of the skeleton due to acceleration of chondrocyte hypertrophy, but overexpression of *HDAC4* in proliferative chondrocytes inhibited chondrocyte hypertrophy [15].

Our previous study indicated that the cartilage of patients with OA had decreased expression of HDAC4 but increased expression of Runx-2, MMP-13, and Col X [17]. This is likely because a decrease of endogenous HDAC4 contributes to the increase of these proteins in OA chondrocytes [17]. Other studies reported that the expression of Runx-2, MMP-13, and type X collagen were greater during the early stages of OA [8,25,26] and that the upregulation of Runx-2 is related to the increased levels of MMP-13 and Col X in an animal model of OA and in the chondrocytes of humans with OA [27,28]. The activated form of MMP-13 degrades components of the ECM and targets type II collagen and proteoglycans [29]. These previous studies thus suggest that downregulation of HDAC4 contributes to the pathogenesis of cartilage degeneration in OA. This led to our hypothesis that increasing the level of HDAC4 during the early stages of OA will slow disease progression.

IL-1β is a critical mediator of OA progression [30]. In this study, we constructed an *in vitro* OA model by stimulating rat chondrocytes with IL-1β. This led to decreased expression of *Col II*, but increased expression of *col X*, *Runx-2* and *MMP-13*. The same altered pattern of gene expression occurs during OA [17,31]. Thus, we initially used this *in vitro* model of OA to investigate the protective effects of *HDAC4* on rat chondrocytes. Our results demonstrated that overexpression of *HDAC4* ameliorated the effects of IL-1β in rat chondrocytes.

We further studied the therapeutic effect of HDAC4 on OA *in vivo* using an established OA rat model, in which OA was induced by ACLT. We then used an adenoviral vector to transfer *HDAC4* into the rat knee. Previous research reported that recombinant adenoviral vectors efficiently transduce genes in this rat model of OA [32]. Our results are in agreement with these previous studies. In particular, we observed expression of HDAC4 at 3 days after injection, with greater expression at 2 weeks but decreased expression at 3 weeks. These findings are consistent with a previous report which found that adenoviral-mediated gene expression is only sustained for 1 month [33]. Thus, to maintain expression of *HDAC4* in articular cartilage, we injected the adenoviral vector every 3 weeks during subsequent experiments. Our results also indicated that the level of *HDAC4* was 8.87-fold higher in the Ad-*HDAC4* group than in the Ad-*GFP* group at 2 weeks.

X-ray examination of rat knees showed that the Ad-*HDAC4* group had fewer osteophytes and a smoother articular surface than the Ad-*GFP* group. The India ink staining results showed less staining of the femoral condyle and tibial plateau cartilage in the Ad-*HDAC4* group than in the Ad-*GFP* group. Because the major pathological features of OA are progressive damage of articular cartilage, osteophyte formation, and changes in periarticular bone [34], our radiological and morphological results demonstrate that *HDAC4* upregulation attenuated articular cartilage degradation.

We confirmed the chondroprotective effect of HDAC4 by Safranin O/Fast Green staining, which showed stronger staining in the Ad-*HDAC4* group than in the Ad-*GFP* group. The Safranin O stain is specific for cartilage glycosaminoglycans and proteoglycans, and is widely used to detect proteoglycan loss in cartilage [35]. Thus, *HDAC4* transduction decreased the loss of ACAN in articular cartilage. The OARSI grading score that we used is a semi-quantitative method that evaluates articular cartilage damage [22]. We found significantly lower OARSI scores (less damage) in the Ad-*HDAC4* group than in the Ad-*GFP* group.

HDAC4 inhibits the transcription of *Runx-2* and *MMP-13* by repressing their promoters [17]. In the present study, we detected Runx-2 by IHC and RT-qPCR. The results of both methods showed there were fewer Runx-2-positive chondrocytes in the Ad-*HDAC4* group than in the Ad-*GFP* group. In addition, *Runx-2* expression was lower in the Ad-*HDAC4* group than in the Ad-*GFP* group. We measured MMP-13 using FMT, IHC, real-time qPCR, and ELISA. FMT is an advanced and sensitive bio-imaging method that provides noninvasive, deep tissue imaging, and quantification of biological targets *in vivo* [36]. Our FMT results showed that MMPs were downregulated in the Ad-*HDAC4* group

relative to the Ad-*GFP* group. This result is consistent with the aforementioned results from IHC, RT- qPCR, and ELISA experiments. In addition to decreased Runx-2 and MMP-13, Col X was also decreased in the Ad-*HDAC4* group relative to the Ad-*GFP* group, based on IHC and RT-qPCR. All these results demonstrate that HDAC4 attenuates the damage of articular cartilage by inhibiting the expression of Runx-2, MMP-13, and Col X *in vivo*.

Our IHC and RT-qPCR data confirmed the upregulation of ACAN and Col II in the Ad-*HDAC4* group relative to the Ad-*GFP* group. Thus, HDAC4 upregulation inhibits catabolism and also increases anabolism. Although the increase of Col II and ACAN suggest that HDAC4 may promote cartilage repair, the mechanism by which HDAC4 enhances this function is not clear, and this topic should be examined in future studies.

In summary, our results demonstrated that HDAC4 attenuated articular cartilage damage and OA progression by repression of Runx-2, MMP-13, and Col X and by induction of collagen II and ACAN in this rat model of OA. These findings suggest that upregulation of HDAC4 may possibly provide chondroprotective effects in patients with early-stage OA.

Supplementary data to this article can be found online at https://doi.org/10.1016/j.intimp.2019.105752.

Funding

This research was funded by National Natural Science Foundation of China [Grant No. 81772415], National Science Foundation for Young Scientists of China [Grant No. 81601949], National International Science and Technology Cooperation Project [Grant No. 2015DFA33050], and the Osteoarthritis Biological Sample Resource Sharing Service Platform Construction Project of Shanxi Province [Grant No. 201705D121010].

Declaration of Competing Interest

The authors declare no conflict of interest.

References

[1] T. Neogi, Y. Zhang, Epidemiology of osteoarthritis, Rheum. Dis. Clin. N. Am. 39 (1) (2013) 1–19, https://doi.org/10.1016/j.rdc.2012.10.004.
[2] D.J. Hunter, S. Deborah, C. Emily, The individual and socioeconomic impact of osteoarthritis, Nat. Rev. Rheumatol. 10 (7) (2014) 437–441, https://doi.org/10.1038/nrrheum.2014.44.
[3] V.L. Johnson, D.J. Hunter, The epidemiology of osteoarthritis, Best Pract. Res. Clin. Rheumatol. 28 (1) (2014) 5–15, https://doi.org/10.1016/j.berh.2014.01.004.
[4] T. Kirsch, B. Swoboda, H.D. Nah, Activation of annexin II and V expression, terminal differentiation, mineralization and apoptosis in human osteoarthritic cartilage, Osteoarthr. Cartil. 8 (4) (2000) 294–302, https://doi.org/10.1053/joca.1999.0304.
[5] D. Pfander, B. Swoboda, T. Kirsch, Expression of early and late differentiation markers (proliferating cell nuclear antigen, syndecan-3, annexin VI, and alkaline phosphatase) by human osteoarthritic chondrocytes, Am. J. Pathol. 159 (5) (2001) 1777–1783, https://doi.org/10.1016/s0002-9440(10)63024-6.
[6] Z. Congming, W. Xiaochun, C. Chongwei, C. Kun, L. Yongping, J. Qiang, D. Juan, Z. Jingming, B.C. Fleming, C. Qian, Indian hedgehog in synovial fluid is a novel marker for early cartilage lesions in human knee joint, Int. J. Mol. Sci. 15 (5) (2014) 7250–7265, https://doi.org/10.3390/ijms15057250.
[7] T. Orfanidou, D. Iliopoulos, K.N. Malizos, A. Tsezou, Involvement of SOX-9 and FGF-23 in RUNX-2 regulation in osteoarthritic chondrocytes, J. Cell. Mol. Med. 13 (9b) (2010) 3186–3194, https://doi.org/10.1111/j.1582-4934.2009.00678.x.
[8] F. Wei, J. Zhou, X. Wei, J. Zhang, B.C. Fleming, R. Terek, M. Pei, Q. Chen, T. Liu, L. Wei, Activation of Indian hedgehog promotes chondrocyte hypertrophy and upregulation of MMP-13 in human osteoarthritic cartilage, Osteoarthr. Cartil. 20 (7) (2012) 755–763, https://doi.org/10.1016/j.joca.2012.03.010.
[9] S. Takeda, J.P. Bonnamy, M.J. Owen, P. Ducy, G. Karsenty, Continuous expression of Cbfa1 in nonhypertrophic chondrocytes uncovers its ability to induce hypertrophic chondrocyte differentiation and partially rescues Cbfa1-deficient mice, Genes Dev. 15 (4) (2001) 467–481, https://doi.org/10.1101/gad.845101.
[10] Z. Qiping, Z. Guang, M. Roy, C. Yuqing, G.R. Xavier, L. Brendan, Type X collagen gene regulation by Runx2 contributes directly to its hypertrophic chondrocyte-specific expression in vivo, J. Cell Biol. 162 (5) (2003) 833–842, https://doi.org/10.1083/jcb.200211089.
[11] S. Dominique, D.J. Behonick, O. Nathalie, H. Babette, H. Bettina, Y. Ying, A.J. Fosang, S.K. Marina, A. Peter, W. Zena, Altered endochondral bone development in matrix metalloproteinase 13-deficient mice, Development 131 (23) (2004) 5883–5895, https://doi.org/10.1242/dev.01461.
[12] D.J. Behonick, X. Zhiqing, L. Shirley, J.M. Buckley, J.C. Lotz, R.S. Marcucio, W. Zena, M. Theodore, C. Céline, Role of matrix metalloproteinase 13 in both endochondral and intramembranous ossification during skeletal regeneration, PLoS One 2 (11) (2007) e1150, , https://doi.org/10.1371/journal.pone.0001150.
[13] W. Fischle, S. Emiliani, M.J. Hendzel, T. Nagase, N. Nomura, W. Voelter, E. Verdin, A new family of human histone deacetylases related to Saccharomyces cerevisiae HDA1p, J. Biol. Chem. 274 (17) (1999) 11713–11720, https://doi.org/10.1074/jbc.274.17.11713.
[14] W. Fischle, V. Kiermer, F. Dequiedt, E. Verdin, The emerging role of class II histone deacetylases, Biochem. Cell Biol. 79 (3) (2001) 337–348, https://doi.org/10.1139/bcb-79-3-337.
[15] R.B. Vega, M. Koichi, O. Junyoung, A.C. Barbosa, Y. Xiangli, M. Eric, M.A. John, P. Chris, J.M. Shelton, J.A. Richardson, Histone deacetylase 4 controls chondrocyte hypertrophy during skeletogenesis, Cell 119 (4) (2004) 555–566, https://doi.org/10.1016/j.cell.2004.10.024.
[16] S. Emi, S. Nagarajan, J.J. Westendorf, E.N. Olson, N.C. Partridge, HDAC4 represses matrix metalloproteinase-13 transcription in osteoblastic cells, and parathyroid hormone controls this repression, J. Biol. Chem. 285 (13) (2010) 9616–9626, https://doi.org/10.1074/jbc.m109.094862.
[17] C. Kun, W. Lei, Z. Zhiqiang, G. Li, Z. Congming, L. Yongping, S. Changqi, S. Xiaojuan, W. Shaowei, L. Pengcui, Decreased histone deacetylase 4 is associated with human osteoarthritis cartilage degeneration by releasing histone deacetylase 4 inhibition of runt-related transcription factor-2 and increasing osteoarthritis-related genes: a novel mechanism of human osteoarthirtis, Arthritis Res. Ther. 16 (6) (2014) 491, https://doi.org/10.1186/s13075-014-0491-3.
[18] A. Gartland, J. Mechler, A. Mason-Savas, C.A. MacKay, G. Mailhot, S.C. Marks Jr., P.R. Odgren, In vitro chondrocyte differentiation using costochondral chondrocytes as a source of primary rat chondrocyte cultures: an improved isolation and cryopreservation method, Bone 37 (4) (2005) 530–544, https://doi.org/10.1016/j.bone.2005.04.034.
[19] G.D. Jay, B.C. Fleming, B.A. Watkins, K.A. Mchugh, S.C. Anderson, L.X. Zhang, E. Teeple, K.A. Waller, K.A. Elsaid, Prevention of cartilage degeneration and restoration of chondroprotection by lubricin tribosupplementation in the rat following anterior cruciate ligament transection, Arthritis Rheum. 62 (8) (2010) 2382–2391, https://doi.org/10.1002/art.27550.
[20] N. Vasilis, B. Christoph, W. Ralph, Fluorescence imaging with near-infrared light: new technological advances that enable in vivo molecular imaging, Eur. Radiol. 13 (1) (2003) 195–208, https://doi.org/10.1007/s00330-002-1524-x.
[21] J.D. Peterson, T.P. Labranche, K.O. Vasquez, S. Kossodo, M. Melton, R. Rader, J.T. Listello, M.A. Abrams, T.P. Misko, Optical tomographic imaging discriminates between disease-modifying anti-rheumatic drug (DMARD) and non-DMARD efficacy in collagen antibody-induced arthritis, Arthritis Res. Ther. 12 (3) (2010) R105, https://doi.org/10.1186/ar3038.
[22] P.H.K. Pritzker, A.S. Jimenez, Ostergaard, J.P. Pelletier, Osteoarthritis cartilage histopathology: grading and staging, Osteoarthr. Cartil. 14 (1) (2006) 13–29, https://doi.org/10.1016/j.joca.2005.07.014.
[23] W. Lei, B.C. Fleming, S. Xiaojuan, T. Erin, W. Wesley, G.D. Jay, K.A. Elsaid, L. Junming, J.T. Machan, C. Qian, Comparison of differential biomarkers of osteoarthritis with and without posttraumatic injury in the Hartley guinea pig model, J. Orthop. Res. 28 (7) (2010) 900–906, https://doi.org/10.1002/jor.21093.
[24] G. Du, H. Zhan, D. Ding, S. Wang, X. Wei, F. Wei, J. Zhang, B. Bilgen, A.M. Reginato, B.C. Fleming, Abnormal mechanical loading induces cartilage degeneration by accelerating meniscus hypertrophy and mineralization after ACL injuries in vivo, Am. J. Sports Med. 44 (3) (2016) 652–663, https://doi.org/10.1177/0363546515621285.
[25] D.N. Clements, S.D. Carter, J.F. Innes, W.E. Ollier, P.J. Day, Analysis of normal and osteoarthritic canine cartilage mRNA expression by quantitative polymerase chain reaction, Arthritis Res. Ther. 8 (6) (2006) R158, https://doi.org/10.1186/ar2053.
[26] J.R. Matyas, A. Lynne, I. Mirela, D.R. Eyre, P.A. Robin, Analysis of cartilage biomarkers in the early phases of canine experimental osteoarthritis, Arthritis Res. Ther. 50 (2) (2014) 543–552, https://doi.org/10.1002/art.20027.
[27] S. Kamekura, Y. Kawasaki, K. Hoshi, T. Shimoaka, H. Chikuda, Z. Maruyama, T. Komori, S. Sato, S. Takeda, G. Karsenty, Contribution of runt-related transcription factor 2 to the pathogenesis of osteoarthritis in mice after induction of knee joint instability, Arthritis Rheum. 54 (8) (2010) 2462–2470, https://doi.org/10.1002/art.22041.
[28] A. Higashikawa, T. Saito, T.S. Kamekura, N. Kawamura, A. Kan, Y. Oshima, S. Ohba, N. Ogata, K. Takeshita, K. Nakamura, Identification of the core element responsive to runt-related transcription factor 2 in the promoter of human type x collagen gene, Arthritis Rheum. 60 (1) (2010) 166–178, https://doi.org/10.1002/art.24243.
[29] T. Shiomi, V.A.J. Lemaitre, Y. Okada, Matrix metalloproteinases, a disintegrin and metalloproteinases, and a disintegrin and metalloproteinases with thrombospondin motifs in non-neoplastic diseases, Pathol. Int. 60 (7) (2010) 477–496, https://doi.org/10.1111/j.1440-1827.2010.02547.x.
[30] X. Ying, X. Chen, S. Cheng, Y. Shen, L. Peng, H.Z. Xu, Piperine inhibits IL-beta induced expression of inflammatory mediators in human osteoarthritis chondrocyte, Int. Immunopharmacol. 17 (2) (2013) 293–299, https://doi.org/10.1016/j.intimp.2013.06.025.
[31] Q. Liu, X. Zhang, L. Dai, X. Hu, J. Zhu, L. Li, C. Zhou, Y. Ao, Long noncoding RNA related to cartilage injury promotes chondrocyte extracellular matrix degradation in osteoarthritis, Arthritis Rheum. 66 (4) (2014) 969–978, https://doi.org/10.1002/art.38309.
[32] J. Hsieh, P.C. Shen, A.L. Shiau, C.L. Wu, C.H. Lee, I.M. Jou, C.R. Wang, J. Chao, L. Chao, M.L. Teo, Adenovirus-mediated Kallistatin gene transfer ameliorates

disease progression in a rat model of osteoarthritis induced by anterior cruciate ligament transection, Hum. Gene Ther. 20 (10) (2009) 1173–1174, https://doi.org/10.1089/hum.2008.096.

[33] M.Z.C. Ruan, E. Ayelet, G. Kilian, D. Brian, B. Terry, C. Yuqing, J. Ming-Ming, Y. Jason, G. Francis, B.H.L. Lee, Proteoglycan 4 expression protects against the development of osteoarthritis, Osteoarthr. Cartil. 21 (176) (2013) S18, https://doi.org/10.1016/j.joca.2013.02.058.

[34] W. Meina, S. Jie, J. Hongting, I. Hee-Jeong, S. John, C. Di, Recent progress in understanding molecular mechanisms of cartilage degeneration during osteoarthritis, Ann. N. Y. Acad. Sci. 1240 (1) (2015) 61–69, https://doi.org/10.1111/j.1749-6632.2011.06258.x.

[35] N. Gerwin, A.M. Bendele, S. Glasson, C.S. Carlson, The OARSI histopathology initiative - recommendations for histological assessments of osteoarthritis in the rat, Osteoarthr. Cartil. 18 (Suppl. 3) (2010) S24–S34, https://doi.org/10.1016/j.joca.2010.05.030.

[36] Z. Jingming, C. Qian, L. Beate, B.C. Fleming, T. Richard, W. Xiaochun, Z. Ge, W. Shaowei, L. Kai, W. Lei, Disrupting the Indian hedgehog signaling pathway in vivo attenuates surgically induced osteoarthritis progression in Col2a1-CreERT2; Ihhfl/fl mice, Arthritis Res. Ther 16 (1) (2014) R11, https://doi.org/10.1186/ar4437.